



ZnO nanoparticles as an oxidase mimic-mediated flow-injection chemiluminescence system for sensitive determination of carvedilol

Pourya Biparva*, Seyed Mohammad Abedirad*, Sayed Yahya Kazemi

Department of Basic Sciences, Sari Agricultural Sciences and Natural Resources University, P.O. Box 578, Sari, Iran

ARTICLE INFO

Article history:

Received 13 January 2014

Received in revised form

16 June 2014

Accepted 18 June 2014

Available online 3 July 2014

Keywords:

Carvedilol

Flow-injection chemiluminescence

ZnO nanoparticles

Nanocatalyst

Mechanochemical

Luminol

ABSTRACT

A simple, rapid and sensitive method was developed using ZnO nanoparticle (ZnO-NP) amplified flow-injection chemiluminescence to detect carvedilol, a non-cardioselective β -blocker. It has been found that carvedilol strongly inhibits the chemiluminescence of luminol–H₂O₂ catalyzed by ZnO-NPs. Under optimum conditions, a linear working range for carvedilol concentrations from 5×10^{-8} to 1.0×10^{-6} mol L⁻¹ ($r > 0.9894$, $n=8$) was obtained with a detection limit of 3.25×10^{-9} mol L⁻¹. The relative standard deviation for 8 repetitive determinations was less than 2.9% and recoveries of 99% and 102% were obtained. ZnO-NPs were synthesized using a green mechanochemical route. Transmission electron microscopy and x-ray diffraction were used to characterize ZnO-NPs. The method was successfully applied to detect carvedilol in pharmaceutical formulations.

© 2014 Elsevier B.V. All rights reserved.

1. Introduction

Carvedilol, 1-(9H-carbazol-4-yloxy)-3-[2-(2-methoxyphenoxy)ethylamino]propan-2-ol, is a nonselective adrenergic blocking agent with 1-blocking activity indicated for the treatment of hypertension and mild or moderate heart failure of ischemic or cardiomyopathic origin. Its molecular structure is shown in Fig. 1. Carvedilol shows minimal inverse agonist activity when compared with other beta blockers and its use has been shown to decrease morbidity from congestive heart failure [1].

Methods have been introduced to assay the presence of carvedilol in plasma, urine and pharmaceuticals in recent years. These include luminescence [2] HPLC–MS/MS [3], HPLC–fluorimetry [4], differential pulse voltammetry [5], fluorimetry [6,7], and chemiluminescence [8,9]. New attempts to introduce efficient methods are under study.

Chemiluminescence (CL) is a phenomenon in which chemically-generated molecules emit light in excited states. The superior emission of CL has recently been tested for use in biotechnology, industry, medicine, and water treatment plants [10]. The attractiveness of CL techniques lies in their simplicity, rapidity, high sensitivity, low cost of instrumentation and

maintenance, and requiring no background light. Since CL is directly related to the concentration of the reactants, it has been exploited as an ultrasensitive method for quantification and localization of chemical analytes that generate luminescence by participating in the CL reaction. These include CL precursors, catalysts, oxidants, cofactors, sensitizers, enhancers and inhibitors [11–17].

Nanotechnology is rapidly expanding in industry for catalysts, separation, luminescence, synthesis, and sensing [18–22]. Because of their unique chemical and physical characteristics, such as high surface area, activity, and sensitivity, nano-materials are in demand for CL reactions as catalysts, enhancers, energy acceptors and CL resonance energy transfer platforms [23,24].

Zinc oxide nanoparticles (ZnO-NPs) are interesting multifunctional metal oxides that have a variety of applications. ZnO-NPs are polar inorganic crystalline materials with a unique combination of properties, including lack of toxicity, good electrical, optical and piezoelectric behaviors, stability in a hydrogen plasma atmosphere, and low cost. ZnO is a well-known semiconductor with a wide direct band gap (3.37 eV) and a large exciton binding energy of 60 meV at room temperature [25]. ZnO-NPs are widely-used in solar cells, as a luminescent, in drug delivery, as an anti-bacterial in the food industry, in electrical and acoustical devices, gas and chemical sensors, coatings, catalysts, micro-lasers, memory arrays and for biomedical applications [25–29].

The present study developed a novel flow-based CL method to detect carvedilol. This method is based on the inhibition effect of carvedilol on CL of luminol catalyzed by ZnO-NPs. It is introduced

* Corresponding authors. Tel.: +98 1513822655; fax: +98 151 3822567.

E-mail addresses: pb.biparva@sanru.ac.ir (P. Biparva), abediradm@yahoo.com (S.M. Abedirad).

as a simple, rapid and sensitive method to assay the presence of carvedilol in pharmaceuticals.

2. Experimental

2.1. Apparatus

Fig. 2 shows a schematic of flow injection analysis with chemiluminescence (FIA-CL). The samples were pumped to a flow cell using two 10 roller peristaltic pumps and a 6-way injection valve (SupelcoRheodyne Model 5020) with a 900 μL sample injection loop. Polytetrafluoroethylene (PTFE) tubes (1.0 mm id) were used to connect all the components of the flow system. The analyte solutions were introduced into the sample loop by means of a plastic syringe. A R-446 photomultiplier (Hamamatsu, Japan) was employed at -700 V .

The CL signal was recorded using a personal computer and was reported in relative arbitrary units (au). Both the steady state CL and fluorescence studies were done using a Cary-Eclipse fluorescence spectrophotometer (Varian, Australia). The x-ray diffraction (XRD) pattern of final ZnO nanoparticles was done using an X-ray diffractometer (XRD; GBC MMA Instruments, Australia) using Ni-filtered Cu K α radiation ($\lambda_{\text{Cu K}\alpha}=0.15418\text{ nm}$) at 35.4 kV and 28 mA with a scanning speed of $2\theta=10^\circ\text{ min}^{-1}$. The size and morphology of the ZnO nanoparticle catalyst were obtained using a Philips CM10 transmission electron microscope (TEM, Philips, The Netherlands) operated at an accelerating voltage of 100 kV.

2.2. Reagents and materials

A stock solution of luminol (3-amino phthalhydrazide) was prepared by dissolving solid luminol (Sigma, USA) in borax-NaOH buffer with a pH of 11.8 without further purification. Doubly distilled water was used throughout the study. Working solutions of H_2O_2 were prepared daily by diluting 30% (v/v) H_2O_2 (Fluka, Switzerland) in water. The $1 \times 10^{-3}\text{ mol L}^{-1}$ stock solution of carvedilol (Fluka, Switzerland) was prepared in methanol and

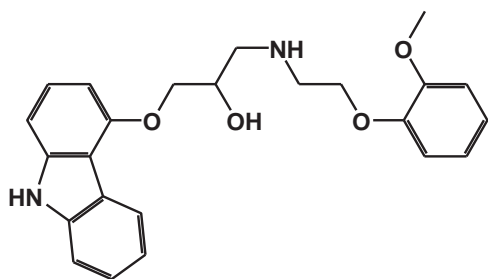


Fig. 1. The molecular structure of carvedilol.

the working standard solutions were prepared by diluting stock solution with H_2O to an appropriate volume. Zinc acetate, oxalic acid and methanol were obtained from Merck (Germany). There was no impurity in ZnO-NPs. They were carefully weighed and then dispersed in the solvent using an ultrasonic water bath to obtain a homogenous solution. Other concentrations were prepared using the stock solution.

2.3. Flow-injection CL detection

As illustrated in Fig. 2, the solutions containing luminol (R_1), ZnO-NPs (R_2), hydrogen peroxide (R_3), and carvedilol or blank solution (R_4) were pumped into flow cells at a flow-rate of 4.5 ml min^{-1} . The concentration of analyte was quantified by measuring the decrease in CL intensity, $\Delta I=I_0-I_s$, where I_0 and I_s are CL intensities in the absence and presence of carvedilol, respectively.

2.4. Assay of sample preparation

Eight tablets containing 6.25 mg carvedilol were weighed and powdered. The equivalent of 6.25 mg carvedilol was weighed with 10 mL methanol and sonicated for 10 min and centrifuged for 10 min. The supernatant was separated and the residue was treated with a fresh portion of 10 mL methanol. The two portions were then mixed and filtered through Millipore membranes of 0.45 μm pore size. Next, 10 mL of the filtered solution was transferred to a flask and increased in volume with ultra-pure water. The same procedure was applied for tablets containing 12.5 mg carvedilol. The final concentrations were 0.625 and 1.25 g mL^{-1} for 6.25 and 12.5 mg tablets, respectively.

3. Results and discussion

3.1. Preparation of ZnO nanoparticles

Anhydrous ZnCl_2 , oxalic acid [$\text{ZnC}_2\text{O}_4 \cdot 2\text{H}_2\text{O}$], and NaCl were the main raw materials. ZnCl_2 and NaCl were thoroughly dried in vacuum at 120°C for 24 h to remove the residual and absorbed water. For typical synthesis, 2 g of dried ZnCl_2 and oxalic acid were put into an agate mortar with a molar ratio of 2:1 and 4 g of NaCl was added to the starting materials as a diluent to form the mixture. The starting materials were mixed and milled for 45 min at room temperature. The precursor was calcined at 450°C in air in a porcelain crucible for 30 min to prepare ZnO-NPs. Removal of the salt by-product was carried out by washing the powder with deionized doubly distilled water and ZnO-NPs were obtained after drying the washed powders [28,30].

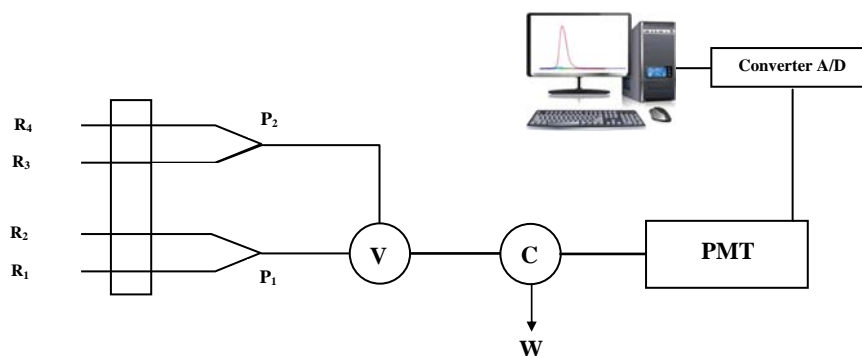


Fig. 2. The diagram of flow-injection system. Schematic diagram of FIA-CL manifold used for the determination of carvedilol. R_1 : luminol solution, R_2 : ZnONPs solution, R_3 : H_2O_2 solution, R_4 : carvedilol or blank solution, P_1 , P_2 : peristaltic pumps, V: injection valve, F: flow cell, and PMT: Photo-multiplier tube.

Fig. 3(a) shows the XRD patterns of washed synthesized zinc oxide powders after calcination. The diffraction angle and intensity of the characteristic peaks of the samples are consistent with that of standard JCPDS Card no. 36-1451. A value of 9.5 nm was calculated from the XRD data for the average size of the mechanochemical synthesized ZnO crystallites using Scherrer's equation. Fig. 3(b) shows TEM micrographs of ZnO-NPs prepared at 450 °C calcination temperature. As the figure shows, the average size of the particles resulting from this method is approximately 5–15 nm. These particle sizes are in good agreement with XRD measurement.

3.2. Enhancement of CL system by nanoparticles

In alkaline media, the oxidation of luminol by hydrogen peroxide induced CL. Fig. 4 shows the effect of ZnO-NPs on CL. In the absence of nanoparticles, a weak CL signal was observed, but the presence of nanoparticles strongly increased the CL. The CL spectra indicated that the maximum emission for both cases was about 425 nm, indicating that the luminophore for CL remained in the excited-state, 3-aminophthalate (3-APA*) [10,14,27,31]. The addition of ZnO-NPs did not lead to the generation of a new luminophore for the luminol system. The strong increase in CL signal confirmed the catalytic role of ZnO-NPs.

3.3. Kinetic study of CL system

The kinetic profile of the CL reaction of luminol–H₂O₂ catalyzed by ZnO-NPs in the presence and absence of carvedilol is shown in

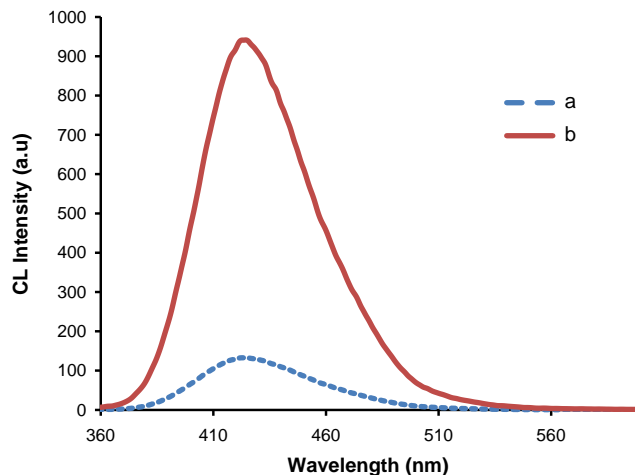


Fig. 4. Steady state CL spectra for the luminol–H₂O₂ in the a) absence (dashed line) and b) presence of ZnO NPs (common line). Experimental condition: luminol (5×10^{-4} mol L⁻¹), H₂O₂ (4×10^{-3} mol L⁻¹), and ZnO NPs (2.5×10^{-5} mol L⁻¹).

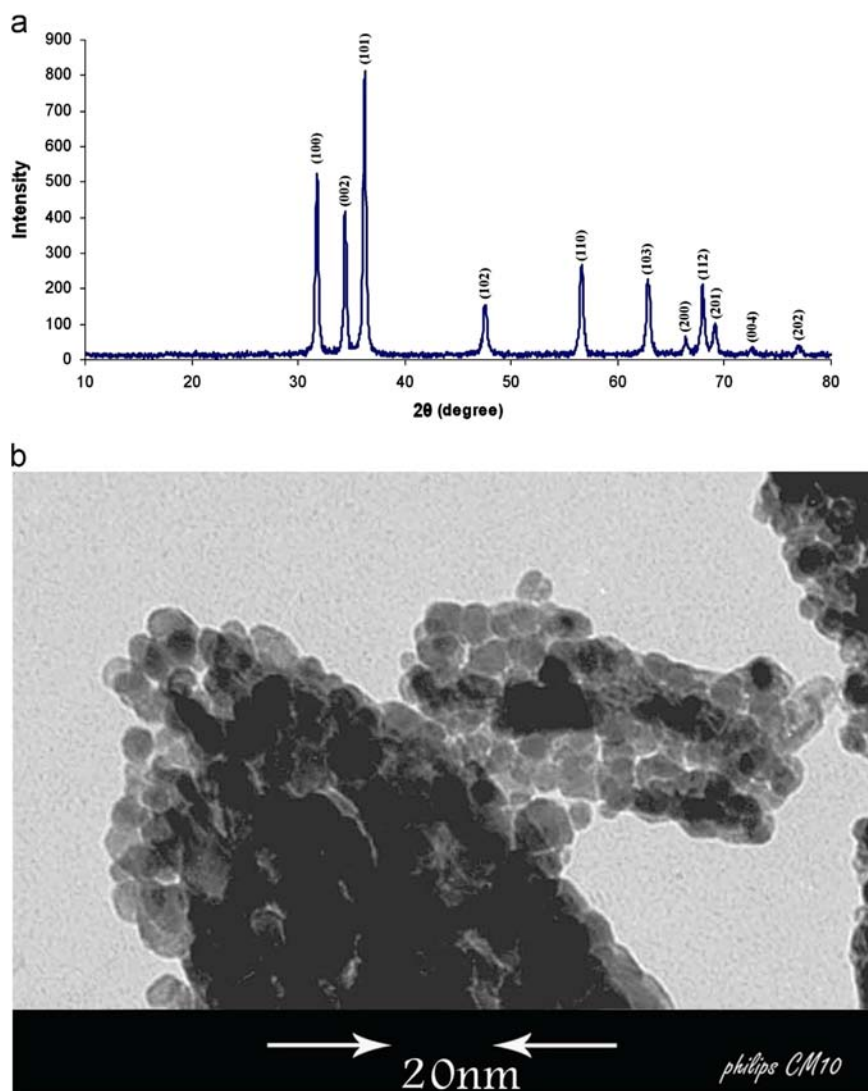


Fig. 3. (a) XRD pattern of ZnO nanoparticles, and (b) TEM micrographs of ZnO nanoparticles calcined at 450 °C in air for 30 min.

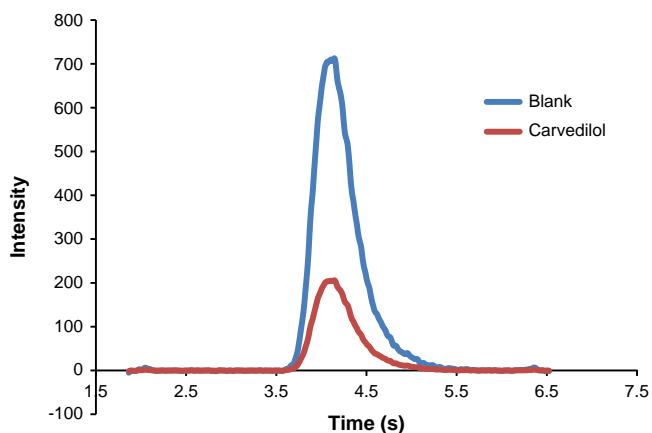


Fig. 5. Chemiluminescence kinetic curves of luminol–H₂O₂–ZnO NPs in the absence and presence of carvedilol. Experimental condition: luminol (6×10^{-4} mol L⁻¹), H₂O₂ (6×10^{-3} mol L⁻¹), ZnO NPs (2.5×10^{-3} mol L⁻¹), pH (11.8), and carvedilol (4×10^{-7} mol L⁻¹).

Fig. 5. As can be seen, in the absence of carvedilol, CL of strong intensity is observed. A significant decrease in the CL signal for luminol–H₂O₂–ZnO-NPs was obtained after injecting carvedilol. The results show that the CL reaction is a flash-type luminescence and the time interval between the onset of CL and its peak is only about 3.6 s. This indicates that the characteristics of the system are suitable for FI-CL determination of carvedilol.

3.4. Possible CL mechanism

The reaction mechanism of oxidation of luminol is believed to involve the superoxide radical O₂^{•-} or the hydroxyl radical OH[•] as the prominent intermediates leading to luminescence [32,33]. Throughout the luminol oxidation process, the presence of oxygen-related radicals (for example, OH[•], O₂^{•-}) as oxidants is expected to occur. For the luminol–H₂O₂ system, oxygen-related radicals are likely generated from H₂O₂. In the absence of a catalyst, the oxidation of luminol by hydrogen peroxide in alkaline solution is a relatively slow reaction and CL intensity is relatively weak. It is assumed that the catalyst ZnO nanoparticles interact with the reactants or the intermediates of the reaction of luminol with hydrogen peroxide.

In the present study, when ZnO nanoparticles were used as catalysts, they catalyzed the decomposition of H₂O₂ to make reactive intermediates such as hydroxyl radicals (OH[•]) and superoxide anions (O₂^{•-}) [27,34]. The resulting products, such as hydroxyl radicals, reacted with luminol to form luminol radicals and diazaquinone, which rapidly reacted with the superoxide anions or monodissociated hydrogen peroxide, giving rise to light emission. This strongly increased emission.

It has been suggested that the O–O bond of H₂O₂ may be broken up into double HO[•] radicals by virtue of the catalysis of ZnO-NPs and the generated hydroxyl radicals are stabilized by ZnO-NPs from partial electron exchange interactions [27,33–35]. The HO[•] radicals react with the luminol anions and HO₂⁻ to facilitate the formation of luminol radicals (L^{•-}) and superoxide radical anions (O₂^{•-}).

Previous studies have reported that molecules with a reducing group react readily with oxygen-containing intermediates [36–38]. The inhibition behavior of carvedilol can be attributed to the competition of carvedilol amino groups with luminol for active oxygen intermediates. Carvedilol interacts with ZnO-NPs to interrupt the formation of luminol radicals (L^{•-}) and superoxide radical anions (O₂^{•-}) taking place on the surface of ZnO-NPs and decreases CL intensity.

3.5. Optimization of factors affecting CL intensity

Fig. 6(a)–(d) show the results of the effect of variables affecting CL intensity. The concentration of luminol, hydrogen peroxide, nanocatalyst, pH, and flow rate provide information that allows optimization of the FIA-CL reaction condition.

3.5.1. Effect of concentration of luminol

Evaluation of luminol concentration at 8×10^{-6} to 2.5×10^{-3} mol L⁻¹ showed an increase in CL intensity as the luminol concentration increased to 6×10^{-4} mol L⁻¹ (Fig. 6(a)). Above this concentration, the CL signal decreased gradually as a result of the self-quenching of luminol. Thus, 6×10^{-4} mol L⁻¹ was selected for all following experiments.

3.5.2. Effect of hydrogen peroxide

Evaluation of the oxidant concentration from 1×10^{-4} to 2×10^{-2} mol L⁻¹ shows that the decrease in CL signal at H₂O₂ concentrations greater than 6×10^{-3} mol L⁻¹ may be a result of fast decomposition of luminol (Fig. 6(b)). A concentration of 6×10^{-3} mol L⁻¹ was thus selected for subsequent experiments.

3.5.3. Effect of concentration of ZnO-NPs

To investigate the effect of catalyst on CL, ZnO-NPs concentration was varied from 1×10^{-6} to 5.5×10^{-5} mol L⁻¹. It was found that an increase in nanoparticles concentration up to 2.5×10^{-5} mol L⁻¹ increased the CL intensity. At higher concentrations, a considerable decrease in intensity was observed. Fig. 6(c) shows the variation in intensity as a function of ZnO-NP concentration.

3.5.4. Effect of pH

The pH of the solution influenced the intensity of the CL reaction. The pH of the buffer solution was varied from 9.5 to 12.5. Maximum CL intensity is obtained at 11.8 in the borax–NaOH buffer solution as indicated in Fig. 6 (d). A pH of 11.8 was thus chosen as the optimum pH.

3.5.5. Effect of flow rate

The effect of flow rate on the CL reaction was also examined. Fig. 6 (e) shows that the relative CL intensity continues to increase as the flow rate increases from 1.0 to 6 mL min⁻¹, probably because the reaction is very fast. A high flow rate may create a strong decrease in the CL signal. A 4.5 mL min⁻¹ flow rate was chosen by considering the sensitivity, reagent consumption and reproducibility.

3.6. Validation method

3.6.1. Analytical performance

A calibration curve was obtained for carvedilol detection by plotting the CL signal versus carvedilol under optimum conditions. This produced a linear range from 5×10^{-8} to 2.0×10^{-6} mol L⁻¹ with a correlation coefficient of 0.9894 ($n=8$). The detection limit was calculated as the amount of carvedilol required to yield a net peak 3 times the standard deviation of the background signal (3σ) and was found equal to 3.25×10^{-9} mol L⁻¹. The relative standard deviation for 8 repetitive detections was less than 2.9%, indicating good reproducibility. LOD (limit of detection) is the compound concentration that produces a signal-to-noise ratio of > 3 and the limit of quantitation (LOQ) is the concentration equal to 10 times the value of the signal-to-noise ratio. LOD and LOQ values for the proposed method based upon these criteria are shown in Table 1.

3.6.2. Analysis of pharmaceuticals

The proposed method was applied to detect the presence of carvedilol in commercial pharmaceutical samples containing 6.25

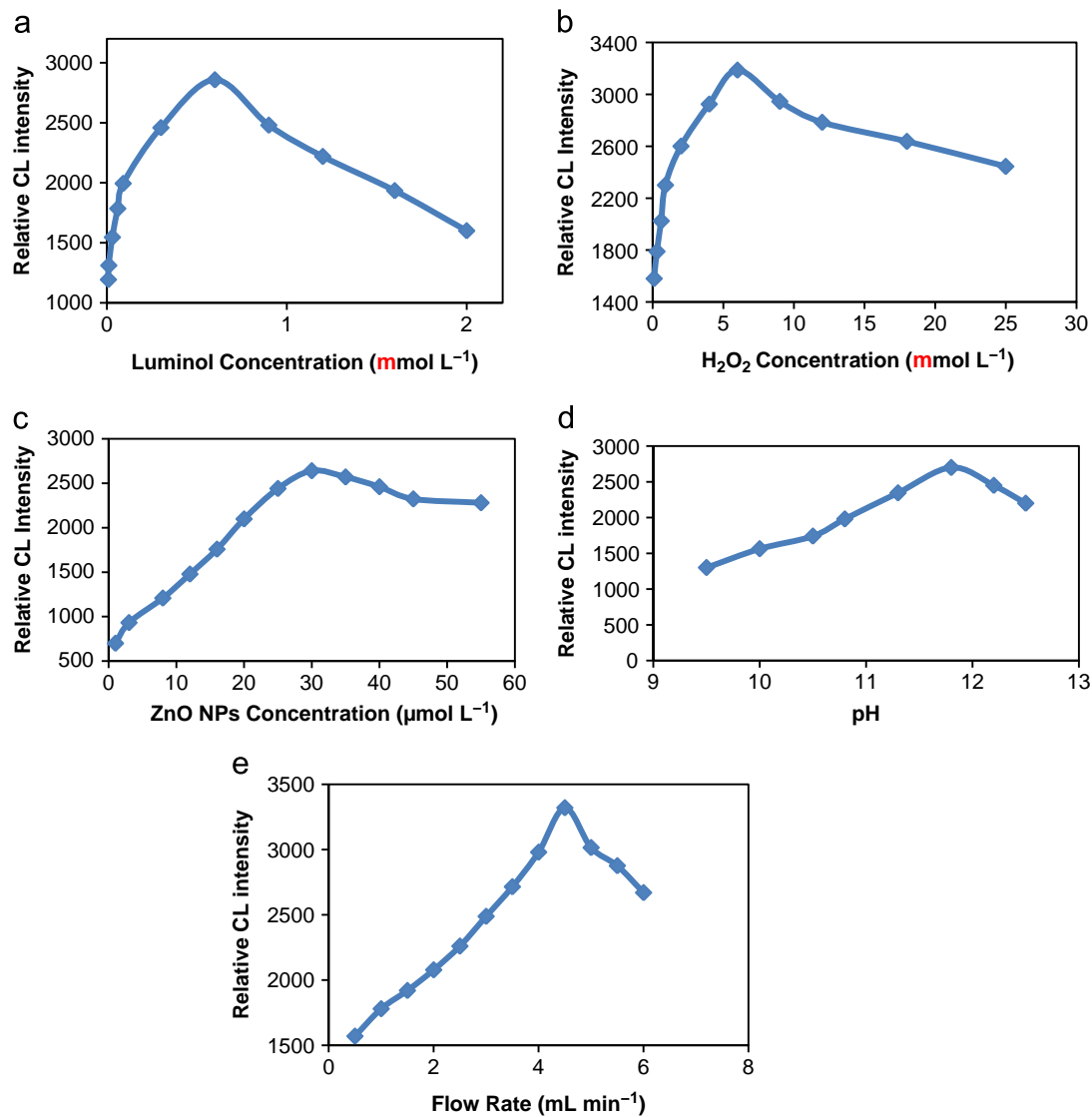


Fig. 6. (a) Effect of luminol concentration on CL intensity, (b) effect of hydrogen peroxide concentration on CL intensity, (c) CL intensity as a function of ZnO NPs, (d) effect of pH on CL intensity, and (e) effect of flow rate on CL intensity.

Table 1

Comparative table for carvedilol determination.

Instrumental methodology	LOD (mol L ⁻¹)	LOQ (mol L ⁻¹)	LOL (mol L ⁻¹)	Samples	Ref.
Luminescence (Tb III complex)	3.2×10^{-7}	1.2×10^{-8}	9.8×10^{-3}	Pharmaceuticals	[2]
HPLC–MS/MS	WD	2.4×10^{-10}	4.9×10^{-7}	Human plasma	[3]
HPLC–fluorimetry	8.8×10^{-10}	3.2×10^{-9}	WD	Rat plasma	[4]
Differential pulse voltammetry	2.4×10^{-8}	6.1×10^{-7}	2.4×10^{-7}	Tablets dosage form	[5]
Synchronous fluorimetry	2.4×10^{-9}	1.2×10^{-8}	2.8×10^{-7}	Medicine dosage	[6]
FI-fluorimetry	3.63×10^{-9}	9×10^{-8}	1×10^{-6}	Pharmaceuticals	[7]
FI-CL (luminol–hypochlorite)	8.7×10^{-9}	1.2×10^{-7}	3×10^{-6}	Pharmaceuticals	[8]
FI-CL ((Ru(bpy) ₃ –KMnO ₄)	6.2×10^{-8}	9.8×10^{-8}	2.5×10^{-6}	Pharmaceuticals	[9]
FI-CL(luminol–ZnO NPs)	3.25×10^{-9}	5×10^{-8}	1×10^{-6}	Pharmaceuticals	This Work

HPLC–MS/MS: high performance liquid chromatography with tandem mass spectroscopy. WD: without datum. FI: flow-injection. LOD: limit of detection. LOQ: limit of quantification. LOL: limit of linearity.

and 12.5 mg of carvedilol, respectively. Recovery rates of about 99% and 102% are obtained at 6.25 and 12.5 mg, respectively, and the results are shown in Table 2. Each concentration was the mean of five determinations and was tested repeatedly for 3–5 consecutive days as a part of inter-day validation.

3.6.3. Interference studies

The interference effect of the coexistence of substances expected to be present in the biological matrices or the pharmaceutical preparation was examined. These substances included ampicillin, hydrochlorothiazide, galactose, lactose, fructose, sucrose, glucose, all

Table 2
Analysis of carvedilol tablets.

Sample (n=8)	Nominal quantity (mg)	Carvedilol found (mg) ^a	Recovery (%)
1	6.25	6.27	100.3
2	6.25	6.30	100.8
3	6.25	6.34	101
4	6.25	6.21	99
5	12.5	12.6	100.8
6	12.5	12.4	99.2
7	12.5	12.8	102
8	12.5	12.4	99.2

^a Mean of five determinations.

of which had no considerable interference effect on the assay of carvedilol.

4. Conclusion

A rapid, simple and sensitive flow-based method has been developed to assay the presence of carvedilol, a non-cardio-selective β -blocker. This method is based on the inhibition effect of carvedilol on the chemiluminescence of luminol. ZnO-NPs were synthesized by a green mechanochemical method and used as a mimic peroxidase catalyst. Under optimum conditions, a linear working range for carvedilol concentrations from 5×10^{-8} to 1.0×10^{-6} mol L⁻¹ ($r > 0.9894$, $n=8$) was obtained with a detection limit of 3.25×10^{-9} mol L⁻¹. This method was applied successfully to detect carvedilol in pharmaceutical formulations.

References

- [1] M. Packer, M.B. Fowler, E.B. Roecker, *Circulation* 106 (2002) 2194–2199.
- [2] I. Leonenko, D. Aleksandrova, A. Yegorova, *Acta Pol. Pharm.* 68 (2011) 325–330.
- [3] N.C.C. Borges, G. Duarte Mendes, D.de Oliveira Silva, V. Marcondes Rezende, R. Barrientos-Astigarraga, G. De Nucci, *J. Chromatogr. B* 822 (2005) 253–262.
- [4] N. Hokama, N. Hobar, H. Kameya, S. Ohshiro, M. Sakanashi, *J. Chromatogr. B* 732 (1999) 233–238.
- [5] A. Radi, T. Elmogy, *II Farm.* 60 (2005) 43–46.
- [6] Y. Xiao, H.Y. Wang, J. Han, *Spectrochim. Acta A* 61 (2005) 567–573.
- [7] R.A. Silva, C.C. Wang, L.P. Fernandez, A.N. Masi, *Talanta* 76 (2008) 166–171.
- [8] C.K. Pires, K.L. Marques, J.L.M. Santos, R.A.S. Lapa, J.L.F.C. Lima, E.A.G. Zagatto, *Talanta* 68 (2005) 239–244.
- [9] N.A. Arfajl, H.H. Abdine, M.A. Sultan, *J. Biomed. Sci.* 3 (2007) 132–137.
- [10] A.M. Garcia-Campana, in: W.R.G. Baeyens (Ed.), *Chemiluminescence in Analytical Chemistry*, Marcel Dekker, New York, 2001.
- [11] K. Aslan, C.D. Geddes, *Chem. Soc. Rev.* 38 (2009) 2556–2564.
- [12] S.Y. Kazemi, S.M. Abedirad, Z. Vaezi, M.R. Ganjali, *Dyes Pigment.* 95 (2012) 751–756.
- [13] S.Y. Kazemi, S.M. Abedirad, S.H. Zali, M. Amiri, *J. Lumin.* 132 (2012) 1226–1231.
- [14] S.Y. Kazemi, S.M. Abedirad, *J. Iran. Chem. Soc.* 10 (2013) 251–256.
- [15] S.Y. Kazemi, S.M. Abedirad, *Spectrochim. Acta A* 118 (2014) 782–786.
- [16] A.M. Garcia-Campana, F.J. Lara, *Anal. Bioanal. Chem.* 387 (2007) 165–169.
- [17] Y.D. Lee, C.K. Lim, A. Singh, J.S. Koh, J. Kim, I.C. Kwon, S. Kim, *ACS Nano* 8 (2012) 6759–6766.
- [18] C.N.R. Rao, Achim Müller, A.K. Cheetham, *The Chemistry of Nanomaterials: Synthesis, Properties and Applications*, Wiley-VCH Verlag GmbH & Co. KGaA, Grünstadt., 2004.
- [19] C.B. Echignac, P. Houdy, M. Lahmani (Eds.), *Nanomaterials and Nanochemistry*, Springer-Verlag, Berlin, Heidelberg, 2007.
- [20] A.A. Matin, P. Biparva, M. Gheshlaghi, K. Farhadi, A. Gheshlaghi, *Chemosphere* 93 (2013) 1920–1926.
- [21] H. Karimi-Maleh, P. Biparva, M. Hatami, *Biosens. Bioelectron.* 48 (2013) 270–275.
- [22] A.A. Matin, P. Biparva, H. Amanzadeh, Khalil Farhadi, *Talanta* 103 (2013) 207–213.
- [23] Q. Li, L. Zhang, J. Li, C. Lu, *Trends Anal. Chem.* 30 (2011) 401–413.
- [24] Y. Su, Y. Xie, X. Hou, Y. Lv, *Appl. Spectrosc. Rev.* 49 (2014) 201–223.
- [25] C. Jagadish, Stephen Pearton (Eds.), *Elsvier*, Amsterdam, London, 2006.
- [26] H. Ming Xion, *Adv. Mater.* 25 (2013) 5329–5335.
- [27] S.F. Li, X.M. Zhang, W.X. Du, Y.H. Ni, X.W. Wei, *J. Phys. Chem. C* 113 (2009) 1046–1051.
- [28] H. Alinezhad, F. Salehian, P. Biparva, *Synth. Commun.* 42 (2012) 102–108.
- [29] S. Shao, K. Zheng, K. Zidek, P. Chabera, T. Pullerits, F. Zhang, *Sol. Energy Mater. Sol. Cells* 118 (2013) 43–47.
- [30] U. Kersen, *Appl. Phys. A* 75 (2002) 559–563.
- [31] R.B. Brundrentt, E.H. White, *J. Am. Chem. Soc.* 96 (1974) 7497–7502.
- [32] G. Merenyi, S.L. Johan, *J. Am. Chem. Soc.* 102 (1980) 5830–5835.
- [33] G. Merenyi, J. Lind, T.E. Erikseon, *J. Biolumin. Chemilumin.* 5 (1990) 53–56.
- [34] Z.F. Zhang, H. Cui, C.Z. Lai, L.J. Liu, *Anal. Chem.* 77 (2005) 3324–3329.
- [35] B. Shahanara, M. Gillian, R. Greenway, A. Wheatley, *Anal. Chim. Acta* 541 (2005) 89–95.
- [36] S.L. Xu, H. Cui, *Luminescence* 22 (2007) 77–87.
- [37] H. Xu, C.F. Duan, C.Z. Lai, M. Lian, Z.F. Zhang, L.J. Liu, H. Cui, *Luminescence* 21 (2006) 195–201.
- [38] A. Safavi, G. Absalan, F. Bamdad, *Anal. Chim. Acta* 610 (2008) 243–248.